

# PRIMARY POLLUTANTS FROM PULSE COMBUSTORS

H.M. Heravi<sup>1</sup>, Bowen P.J.<sup>2</sup> and Syred N.<sup>2</sup>

*Mechanical Engineering Division, Islamic Azad University, Mashhad Branch, Iran*  
[momahedi\\_heravii@yahoo.com](mailto:momahedi_heravii@yahoo.com)

## Abstract

The aim of this study is to improve a phenomenological model for pulsating combustion by predicting characteristics of 'primary pollutants' NO<sub>x</sub> and CO, as well as minor combustion species. The phenomenological thermo-fluid pulse combustor model previously presented has been developed to provide predictions of primary pollutant characteristics through integration with a detailed kinetic mechanism (GRI-Mech 2.11) and a reduced kinetic model, both provided from the CHEMKIN site. Homogeneous methane-air mixtures have been modeled across a range of practical, fuel-lean operating conditions, and predictions of primary pollutants from both models have been compared with available data. Oscillatory characteristics of combustion species are generated, and consistent with published data, the optimum operating conditions of the combustor are predicted to be around equivalence ratio of 0.74, where very low NO<sub>x</sub> and CO are found of only a few ppm. Perhaps surprisingly, compared against experimental data available, the NO<sub>x</sub> and CO predictions utilizing the reduced mechanism apparently provide better agreement than that using the detailed GRI-Mech.2.11.

**Keywords:** Pollutant-Pulse combustor-Modeling

## 1. Introduction

Flames are sensitive to excitation from sound waves with their response dependent upon the amplitude, frequency and nature of acoustic wave impingement. In the Helmholtz pulse combustor, the response to this excitation leads to an increased rate of combustion and thermal efficiency, with associated high rates of heat transfer and reduced pollutant emissions under suitable operating conditions [1-4]. The aim of this research program is to further develop an integrated phenomenological thermo-fluid/chemical kinetic model [5-8] by exploring the effect of detailed chemical kinetic schemes employed ranging from a reduced mechanism (17 reactions), [9] to the developed GRI-Mech 2.11 Scheme (279 reactions)[10], and appraising predictions against published experimental data. The type of pulse combustor considered belongs to the aerovalved family, whose generic operation is non-premixed but has the added practical attraction of providing self-sustaining operation with no mechanical moving parts.

Whilst predictions of NO<sub>x</sub> production due to forced oscillations of the pressure, velocity and heat release within the combustor have been presented previously [4], the novelty of the current approach is that no pulsations are presumed a priori; transient oscillations have been shown to be a natural solution of the simplified first-order coupled time-dependent problem [5]. Hence the time-dependent NO<sub>x</sub> predictions are governed simply by the boundary conditions of the model. A simplified model facilitates numerical experiments capable of isolating and investigating the mechanisms that contribute to reduced NO<sub>x</sub> and CO performance in pulse combustors compared to experimental combustors. The inter-relation between the physics and chemistry that govern the operation of pulse combustors is complex and involves complex fluid flows with associated mixing issues, chemical kinetics, turbulent combustion, heat transfer, thermo-acoustic coupling, etc. Although development of 3-dimensional transient CFD combustion models are necessary to provide detailed analysis of the influence of fluid dynamic effects on mixing and combustion, the role of the simplified phenomenological model is in providing relatively fast predictions and a 'transparency' which allows scientific interpretation of predictions. Here the transient nature of operation is afforded higher priority than spatial variations; hence this model provides spatially averaged, time-based predictions.

The construction of a premixed version of the model has been described elsewhere [6]. This basic model was first improved to facilitate non-premixed operation, more representative of aerovalved operation [7, 8], and then

---

1. Assistant Professor, Combustion & Energy.

2. Professor, Combustion & Energy, Cardiff University, UK.

recently integrated with a reduced chemical kinetic scheme (using the CHEMKIN suite) [9] to provide the first predictions of primary pollutants  $\text{NO}_x$  and  $\text{CO}$  from this type of phenomenological model [11]. Here, the sensitivity of these predictions to the type of chemical-kinetic scheme utilized are explored by generating and utilizing a pulse-combustor model integrated with the GRI-Mech 2.11 [10] scheme for methane.

## 2. Physical and Chemical Model Integration

The thermo-fluid model of the combustion chamber was originally based on the thermal model proposed by Richards et al. [5], and was previously modified to include separate oscillating air and fuel inlet characteristics [7, 8, 12]. A schematic of the model geometry is shown in Figure 1.

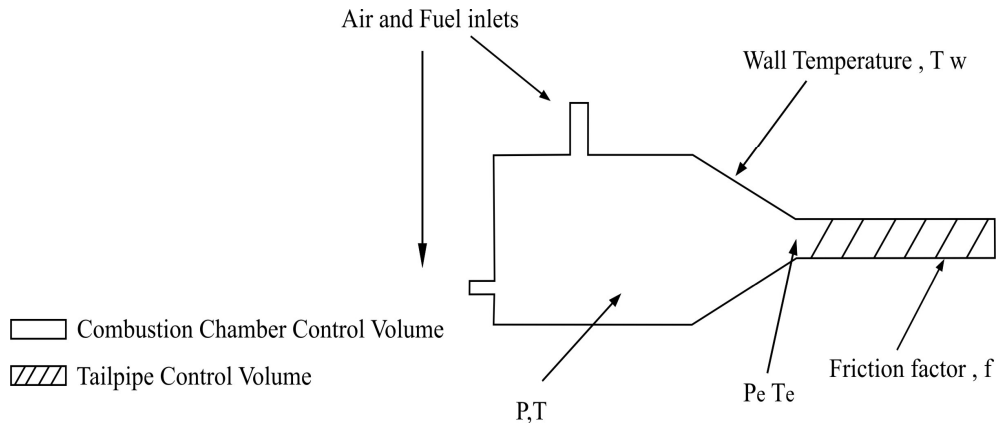


Fig. 1 Schematic of the control volume geometry

The model geometry, which determines the frequency characteristics, is based on an experimental aerovalved pulse combustor [13]. The transient, spatially averaged thermodynamic model is based on the energy equation within the combustor chamber control volume, coupled with a simple fluid dynamic sub-model for the tail pipe. The model is described in detail elsewhere [7, 12]. Also, at this stage of development, a mixing timescale has not been included, and so the model is akin to a perfectly-stirred reactor and dominated by chemical kinetics, though the importance mixing timescales is fully appreciated within the limits of aerovalved operation. The formulation of the original model [5] developed from the energy balance rendered it incapable of non-premixed operation, which is one of the dominant characteristics of aerovalved operation and was also only valid for near-stoichiometric conditions. For the improved model, equations for fuel and oxidant species as functions of time within the combustor are treated independently within the Runge-Kutta numerical solution scheme. It is envisaged that the next stage will incorporate a mixing timescale to more accurately reflect the aerovalved process.

The main focus of this research has been to compare predictions, particularly predictions of primary pollutants, from the pulse combustor model integrated with a reduced chemical kinetic scheme, compared with those from a detailed kinetic mechanism. This is perceived to be one advantage of the phenomenological model over more detailed CFD models, in that its relative simplicity facilitates integration with chemical kinetic schemes of greater detail than is usually possible. The chemistry modeling has been undertaken using the commercially available CHEMKIN II [14] package, more specifically, the SENKIN program. SENKIN predicts the time-dependent chemical kinetic behavior of a homogeneous gas phase mixture in a closed system. This code is linked to the pulse combustor model at each time step to predict the mole fractions of the species. The reduced mechanism was based on the work of Sung et al [9], and describes the methane oxidation chemistry in terms of 17 elementary reactions involving 21 species. The detailed mechanism employed via the GRI-Mech 2.11 [10] by comparison employs 49 species and 279 reactions. Thermodynamic properties used in this study were obtained from the CHEMKIN thermodynamic database. The transient thermo-fluid results are presented in terms of the combustor pressure and temperature, and the chemical species predictions are presented in terms of primary reactants,  $\text{CH}_4$  and  $\text{O}_2$ , primary combustion products,  $\text{H}_2\text{O}$  and  $\text{CO}_2$ , various influential minor chemical species, and the primary combustion pollutants,  $\text{CO}$  and  $\text{NO}_x$ . Results are presented for the constant heat transfer coefficient and the predictions are appraised against the time-averaged  $\text{CO}$  and  $\text{NO}_x$  predictions of Keller et al. [2,15].

A simple aerovolved pulse combustor can be modeled [8,12] via five normalized ordinary differential equations. The first differential equation describes the normalized temperature (thermal energy balance) over the combustion chamber and become

$$\frac{d\tilde{T}}{dt} = \gamma \left\{ \frac{1}{\tau_f} + \frac{1}{\tau_{HT}} + \frac{1}{\tau_c} \right\} \frac{\tilde{T}}{\tilde{P}} - \left\{ (\gamma-1) \frac{Z_e}{\rho_0} + \frac{1}{\tau_f} + \frac{\gamma T_0}{\tau_{HT} T_w} \right\} \frac{\tilde{T}^2}{\tilde{P}} \quad (1)$$

Where  $Z_e$  is the ratio of exit mass flow rate to the combustion chamber volume,  $T_w$  is wall temperature,  $T_0$  is the ambient temperature,  $\tau_f$  is the characteristic flow time,  $\tau_{HT}$  is the characteristic heat transfer time, and  $\tau_c$  is the characteristic combustion time. Combining a mass balance with equation (1) results in an equation describing the time variation of the normalized pressure in the combustion chamber:

$$\frac{d\tilde{P}}{dt} = \gamma \left\{ \frac{1}{\tau_f} + \frac{1}{\tau_{HT}} + \frac{1}{\tau_c} \right\} - \left\{ \frac{Z_e}{\rho_0} + \frac{T_0}{\tau_{HT} T_w} \right\} \gamma \tilde{T} \quad (2)$$

In order to solve equations (1) and (2) a combustion model, the characteristic combustion time in terms of instantaneous heat release per unit volume needs to be defined. Therefore, in addition to the total mass balance equations, one can write equations for the rate of change of the fuel and oxygen in the combustion chamber respectively:

$$\frac{dY_f}{dt} = (Y_{f,i} - Y_f) \frac{\tilde{T}}{\tilde{P}} \frac{1}{\tau_f} + Y_f \frac{\tilde{T}}{\tilde{P}} \frac{Z_e}{\rho_0} - \frac{\tilde{T}}{\tilde{P}} \left( \frac{C_p T_0}{\Delta H_f} \right) \frac{1}{\tau_c} \quad (3)$$

$$\frac{dY_0}{dt} = (Y_{0,i} - Y_0) \frac{\tilde{T}}{\tilde{P}} \frac{1}{\tau_f} + Y_0 \frac{\tilde{T}}{\tilde{P}} \frac{Z_e}{\rho_0} - Y_{0,e} \dot{m}_e \frac{\tilde{T}}{\tilde{P}} \frac{1}{\rho_0 V} - S_r \frac{\tilde{T}}{\tilde{P}} \left( \frac{C_p T_0}{\Delta H_f} \right) \frac{1}{\tau_c} \quad (4)$$

We need to write the momentum equation for the tail pipe in terms of the rate of tailpipe gas velocity (normalized to the cold flow tailpipe velocity) and is defined as:

$$\frac{d\tilde{u}}{dt} = (\tilde{P}_e - 1) \left( \frac{RT_0 \tau_f}{L_{tp} L_{c2}} \right) \frac{\tilde{T}_e}{\tilde{P}_e} - \frac{L_{c2} f}{2 D_{tp} \tau_f} \frac{\tilde{u}^3}{|\tilde{u}|} \quad (5)$$

Where:

$$\tau_f = \frac{\rho_0}{Z_i} \quad (6)$$

represents a characteristic flow time;

$$\tau_{HT} = \frac{L_{c1} \rho_0 C_p T_0}{h T_w} \quad (7)$$

Represents a characteristic heat transfer time;

$$\tau_c = \frac{\rho_0 C_p T_0}{\dot{Q}} \quad (8)$$

Represents a characteristic combustion time.

Finally, the following equation to express the combustion time is derived by combining equation (7) with the heat release rate per unit area and fuel reaction rate for a single step reaction mechanism in order to solve equations (3) and (4):

$$\frac{1}{\tau_c} = A' \frac{\Delta H_f}{C_p T_0} \frac{\tilde{P}^2}{\tilde{T}^{3/2}} Y_f \frac{Y_0}{S_r} e^{-\tilde{T}_a / \tilde{T}} \quad (9)$$

### 3. Results and Discussion

First, the extended system of equations is solved using the Runge-Kutta scheme for steady inlet conditions in order to determine whether the NO<sub>x</sub> species balance results in a plausible limit cycle solution within the combustor. Figures 2 to 5 show the time series of pressure and temperature oscillations, and the pollutant mole fractions in the combustor section during transient start-up and after steady conditions are established. In these representative figures, the reduced mechanism is employed, the fuel supply is fixed at 0.57 g/s, equivalence ratio 0.85, the Nusselt number is constant, and all pollutant predictions are corrected to 3% O<sub>2</sub>. Figure 2 shows that the limit cycle oscillations stabilize 100 ms after ignition, consistent with the previous models [5-8]. In this representative example, the resulting oscillation frequency is 71.5 Hz and shows good agreement with the operational frequency of the aerovalved combustor test facility upon which the model dimensions are based [13]. The resulting pressure amplitudes are 12.2 kPa with a mean operating temperature of 1600 K. Comparison with Figure 3 shows that pressure and temperature stabilize before the NO<sub>x</sub> concentrations. This is due to the artificial conditions introduced at  $t = 0$ s to invoke the reaction, resulting in unrealistically high NO<sub>x</sub> production at these early stages. However, the NO<sub>x</sub> species equation gradually purges the combustor until limit cycle oscillations are reached with amplitudes about 20% of the mean. For this case, the mean concentration of NO and NO<sub>2</sub> is 11.7 and 0.07 ppm respectively. The very low values of NO<sub>2</sub> can be considered negligible and therefore, for discussion purposes, NO represents the predicted total NO<sub>x</sub> value. Increased pollutant levels are encountered in Figure 4, as the predicted values of CO reach as high as 6000 ppm in the combustor. These high levels of CO reduce to less than 10ppm at the end of the tail pipe.

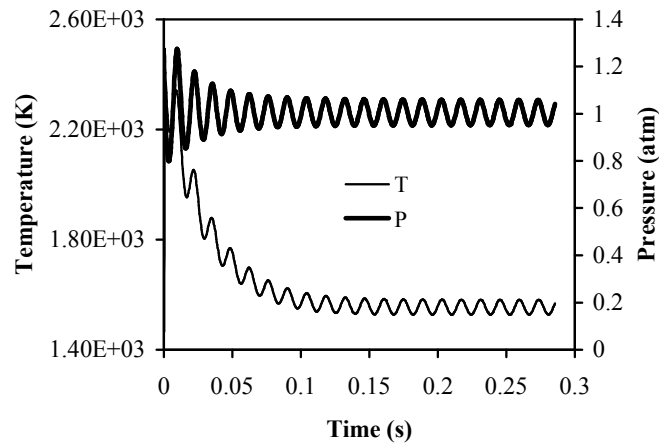


Fig. 2 Pressure and temperature for  $\phi = 0.85$  using reduced scheme.

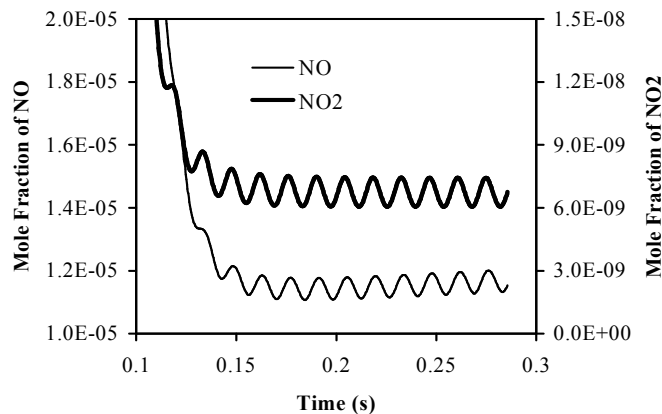


Fig. 3 NO<sub>x</sub> mole fractions for  $\phi = 0.85$  using reduced scheme.

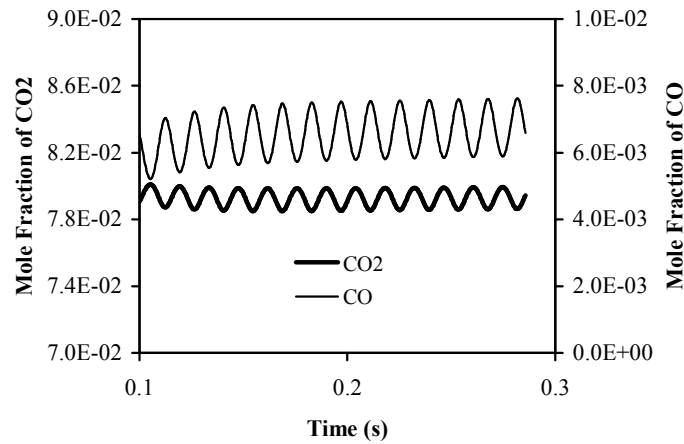


Fig. 4 CO and CO<sub>2</sub> mole fractions using reduced scheme in the combustor

Figure 5 shows the sensitivity of the CO and NO<sub>x</sub> predictions to the influence of the tailpipe. The NO<sub>x</sub> values in combustion chamber and at the exit of the tailpipe remain nearly constant, which means the additional residence time does not affect NO<sub>x</sub> formation. The results also indicate that all the NO<sub>x</sub> production occurs during the combustion process. However, the added fluid residence time in the tailpipe clearly has a strong influence on the predicted CO levels. The concentration CO has reduced from 6000 ppm in the combustion chamber to 4 ppm at the end of tailpipe. The results of Figures 3 to 5 indicate that the NO<sub>x</sub> generation source term and species balance are satisfactorily integrated within the first order coupled system and numerical scheme. Furthermore, the stabilized mean NO<sub>x</sub> concentration of about 11 ppm agrees well with previous literature findings [2, 15, 16, 17]. The NO<sub>x</sub> levels generally oscillate in-phase with the predicted pressure and temperature oscillations, though closer inspection reveals a small phase shift .10° between NO<sub>x</sub> and temperature, whilst being almost precisely in-phase with pressure at this equivalence ratio. With the ability of the integrated model to achieve stable NO<sub>x</sub> oscillations, it is now possible to explore the influence of equivalence ratio on NO<sub>x</sub> production within the lean range where prompt NO<sub>x</sub> becomes the dominant formation mechanism, i.e.  $0.5 < \phi < 0.8$ . To isolate the effect of equivalence ratio, parameters that have been found to influence NO<sub>x</sub> production such as the heat transfer coefficient, wall temperature, and mass flow rate are kept constant.

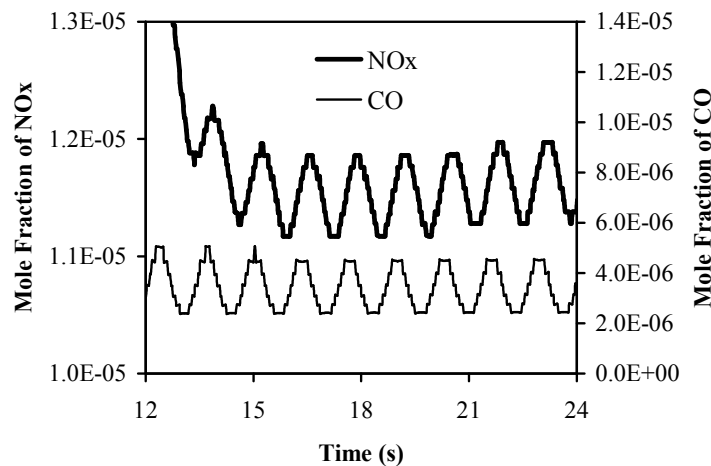


FIG. 5 NO<sub>x</sub> and CO mole fractions for  $\phi=0.85$  at the end of the tailpipe using reduced mechanism

The effects of changing the equivalence ratio on the primary combustion products of O<sub>2</sub>, H<sub>2</sub>O, CO<sub>2</sub> and N<sub>2</sub> using the detailed GRI-Mech 2.11[10] scheme are shown in Figure 6. Reassuringly, increase in the equivalence ratio from  $\phi= 0.7$  towards stoichiometric conditions increases the production of CO<sub>2</sub> and H<sub>2</sub>O, and decreases the production of O<sub>2</sub>, as expected from elementary combustion theory.

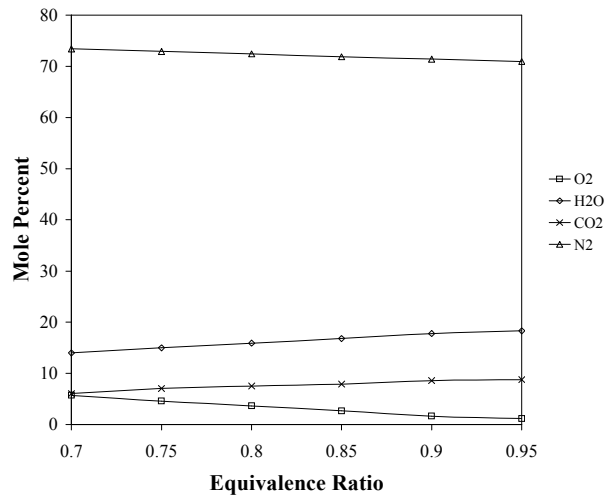


Fig. 6 Mole fraction of primary combustion products for  $\phi = 0.7-0.95$  ( GRI-Mech 2.11)

Figure 7 compares predicted time-averaged values of NO<sub>x</sub> and CO obtained using the reduced mechanism against the experimental data of Keller et al.[15] over a range of practical equivalence ratios. The model predictions agree with the experimental trends qualitatively, and in terms of a quantitative comparison, the NO<sub>x</sub> predictions differ to the experimental data by a few ppm, whilst CO predictions are in a good agreement with the experimental results.

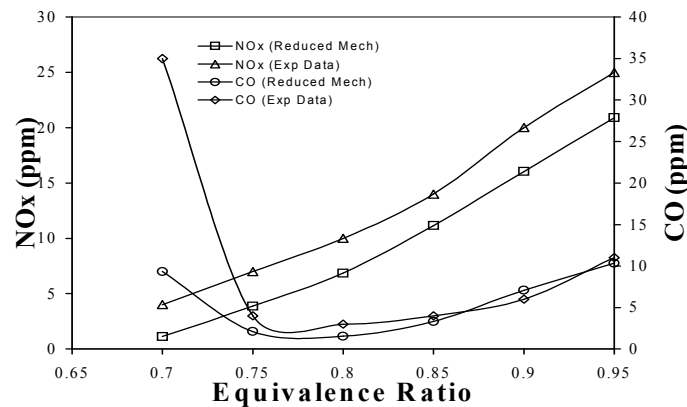


Fig. 7 Comparison of NO<sub>x</sub> and CO predicted by the model and experimental results of Keller et al ( Reduced Mechanism)

Optimal operating conditions in terms of primary pollutant performance can be determined from Figures 8 and 9 for both models, as well as the experimental data. At an equivalence ratio of around 0.74, both NO<sub>x</sub> and CO are less than 10 ppm for both models and the data set. Further reduction in equivalence ratio limits the performance in terms of CO, due to the increase in CO emissions that occurs when approaching  $\phi = 0.7$ , though this characteristic is least prominent for the detailed mechanism. Over the equivalence ratio range 0.73 - 0.8, both NO<sub>x</sub> and CO emissions are under 10 ppm for all three cases. Surprisingly the detailed mechanism compares less favorably with the experimental data of Keller et al [15] than the reduced scheme. Gri Mech 2.11 significantly over predicts CO for equivalence ratios  $> 0.8$ , Fig 8, whilst the reduced mechanism performs well in the same region. The model utilizing GRI-Mech 2.11[10] underpredicts NO<sub>x</sub>, Fig 9, all for equivalence ratios, the reduced mechanism generally performing better. There are many plausible reasons for this finding, including differences between the experimental set-up and the model assumptions, limitations of the phenomenological approach, limitations in the kinetic schemes themselves, etc. Further work is needed to decouple these influences.

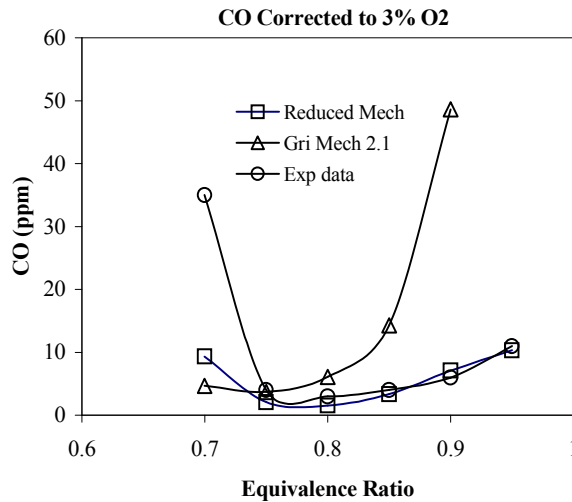


Fig. 8 Comparison of predictions data for CO using GRI-Mech. and reduced mechanism

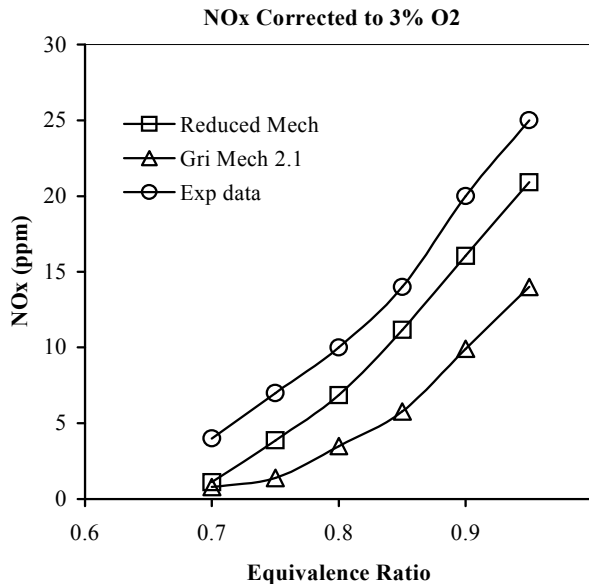


Fig. 8 Comparison of predictions data for NOx using GRI-Mech. and reduced mechanism

#### 4. Conclusions

- Primary pollutants NOx and CO have been predicted from a phenomenological pulse combustor model for the first time. The relative simplicity of the thermo fluid model employed has the advantage over a more rigorous Navier Stokes solution that detailed chemical kinetic models can be readily employed within the integrated model.
- A detailed kinetic mechanism (GRI-Mech 2.11) [10] and reduced mechanism [9] (utilizing 21 species and 17 reactions) have each been coupled with the thermo fluid model at each time-step, providing two integrated thermal pulse combustor models. The usual oscillatory behavior of pressure and temperature with the addition of combustion species is predicted for both integrated models, hence facilitating performance comparison.
- Both integrated models predict pressure, temperature and the species inside combustor, although to predict realistic concentrations of the species at the exit of the tailpipe, the results from the combustor had to be taken as initial conditions to run the model of the tailpipe.

- Both integrated models predict the characteristic 'U-shaped' CO trend predicting CO < 5 ppm at about  $\phi = 0.74$ , whilst increasing as  $\phi$  reduces below 0.7. Both models predict monotonically increasing NO<sub>x</sub> with increase in equivalence ratio.
- Predictions using the reduced mechanism agree with the experimental data and show low concentrations of CO and NO<sub>x</sub> of < 10 ppm attained when  $\phi = 0.74$ . Experimental studies and both models presented now agree that this is the optimal operating range in terms of pollutant performance. However, the CO contribution is very sensitive to further reductions in equivalence ratio, indicating that combustor control is critical in practical lean-burn operation.
- Contrary to expectation, the results from the reduced mechanism provided better quantitative agreement than those from the detailed mechanism for primary pollutants. The possible reasons for this probably arises from the derivation of the reduced mechanism from GRI Mech3, mirrors the experiences of Sung et al [9] and requires further investigation.

## 5. References

1. Zinn, B. T., 'Pulse Combustion: Recent Applications and Research Issues', *Twenty-Fourth Symposium (international) on Combustion*, The Combustion Institute, pp. 1297-1305, 1992.
2. Keller, J. O., and Hongo, I., 'Pulse Combustion: The Mechanisms of NO<sub>x</sub> Production', *Combustion and Flame*, 80: 219-237, 1990.
3. Keller, J. O., Bramlette, T. T., Dec, J. E., and Westbrook, C. K., 'Pulse Combustion: The Importance of Characteristic Times', *Combustion and Flame*, 75: 33-44, 1989.
4. Au-Yeung, H. W., Garner, C. P., and Hanby, V. I., 'Modeling the Effects of Combustion Frequency and Pressure Amplitude on NO Formation in a Gas-Fired Combustor', *J. Inst. Energy*, 1999.
5. Richards, G. A., Morris, G. J., Shaw, D. W., Keeley, S. A., Welter, M. J., 'Thermal Pulse Combustion', *Combust. Sci. and Tech.*, Vol. 94, pp. 57-85, 1993.
6. Marsano, S., Bowen, P.J., and O'Doherty, T., 'Cyclic Modulation Characteristics of Pulse Combustors', *Twenty-Seventh Symposium (International) on Combustion*, The Combustion Institute, pp.3155-3162, 1999.
7. Marsano, S., 'Modeling Transient Combustion Systems', *Ph.D Thesis*, Division of Mechanical Engineering and Energy Studies, Cardiff University, 1999.
8. Marsano, S., Bowen, P.J., and O'Doherty, T., 'Model of an Aerovalved Pulse Combustor', *accepted for publication in Combustion and Flame*.
9. Sung, C. G., Law, C. K., and Chen, J. Y., Augmented Reduced Mechanisms for NO Emission in Methane Oxidation, *Combustion and Flame*, 125:906-919, 2001.
10. Smith, G. P., Golden, D. M., Frenklach, M., Moriarty, N. W., Eiteneer, B., Goldenberg, M., Bowman, C. T., Hanson, R. K., Song, S., Gardiner, W. C., Jr., Lissianski, V. V., and Qin, Z., [http://www.me.berkeley.edu/gri\\_mech/](http://www.me.berkeley.edu/gri_mech/).
11. Heravi H.M., Bowen P.J., Dawson J.R. and Syred N. 'An Integrated Thermo-Fluid, Chemical Kinetic Model for Pulse Combustors', *paper presented at 42nd AIAA Aerospace Sciences Meeting and Exhibit*, Reno (USA), 5-8 January 2004.
12. Heravi, H.M 'Integrated Physical and Chemical Modeling of Pulse Combustors', *Ph.D Thesis*, Division of Mechanical Engineering and Energy Studies, Cardiff University, 2003.
13. Beale, A. J., 'Aerovalved Pulse Combustion', *Ph.D Thesis*, Division of Mechanical Engineering and Energy Studies, Cardiff University, 1999.
14. Kee, R. J., Rupley, F. M., and Miller, J. A., ChemkinII: A Fortran Chemical Kinetic Package for the Analysis of Gas Phase Chemical Kinetics, Sandia National Laboratories Report No., SAND 89-8009, 1989.
15. Keller, J. O., Briollette, T. T., Barr, P. K., and Alvarez, J. R., 'NO<sub>x</sub> and CO Emissions from a Pulse Combustor Operating in a Lean Premixed Mode', *Combustion and Flame*, 99: 460-466, 1994.
16. Corliss, J. M., Putnam, A. A., Murphy, M. J., and Locklin, D. W., 'NO<sub>x</sub> Emissions From Several Pulse Combustors', *105th ASME Winter Annual Meeting*, New Orleans, La., Paper No. 84-JPGC-APC-2, Dec. 1984.
17. Barham, P., David, J Hargreaves, K.J.A., Ipakchi, H., and Maskell, W. C., Sauba, R.N., and Suthenthiran, A 'Characterization of a 5 kW Gas-Fired Pulsed Combustors: NO<sub>x</sub> and CO emissions control II, Institute of Energy , pp 220-238 London, 1995.